

A Calcium Wave Mediated by Gap Junctions Coordinates a Rhythmic Behavior in *C. elegans*

Maureen A. Peters,^{1,3} Takayuki Teramoto,²
 Jamie Q. White,³ Kouichi Iwasaki,²
 and Erik M. Jorgensen^{3,*}

¹Department of Biology
 Oberlin College
 Oberlin, Ohio 44074

²Department of Molecular Pharmacology and Biological
 Chemistry

Northwestern University Medical School
 Chicago, Illinois 60611

³Howard Hughes Medical Institute and the Department
 of Biology
 University of Utah
 Salt Lake City, Utah 84112-0840

Summary

Intercellular calcium waves can be observed in adult tissues, but whether they are instructive, permissive, or even required for behavior is predominantly unknown. In the nematode *Caenorhabditis elegans*, a periodic calcium spike in a pacemaker cell initiates a calcium wave in the intestine [1, 2]. The calcium wave is followed by three muscle contractions that comprise the defecation motor program [1]. Normal wave propagation requires the pannexin gap-junction subunit INX-16 at the interfaces of the intestinal cells. In the absence of this gap-junction subunit, calcium waves are frequently absent. The remaining waves are slow, initiate at abnormal locations, or travel in the opposite direction. Abnormal waves are associated with parallel effects in the first step of the motor program: The contractions of the overlying muscles fail to propagate beyond the pacemaker cell, are slow, initiate in abnormal locations, or are reversed. Moreover, the last two motor steps are predominantly absent. Finally, the absence of this gap-junction subunit also affects the reliability of the pacemaker cell; cycle timing is often irregular. These data demonstrate that pannexin gap junctions propagate calcium waves in the *C. elegans* intestine. The calcium waves instruct the motor steps and regulate the pacemaker cell's authority and reliability.

Results and Discussion

pannexin inx-16 Encodes an Intestinal Gap-Junction Subunit

The defecation cycle is a stereotyped behavior that requires the coordinated activity of the intestine, neurons, and muscle in the nematode [3]. This motor program is repeated with an approximately 45 second periodicity. A critical component of the timekeeping mechanism of this rhythm is the inositol-1,4,5-

trisphosphate (IP₃) receptor [4, 5]. In wild-type animals, cyclic calcium spikes in the posterior intestine directly precede the initiation of the motor program, and these spikes are absent in the IP₃ receptor mutant [5]. The posterior calcium spike initiates a calcium wave that progresses through the intestinal cells; disrupting IP₃ receptor function pharmacologically disrupts the calcium-wave propagation [1, 2]. What is the relationship between the calcium wave and the associated behaviors?

We have identified a mutation, *ox144*, that causes a constipated phenotype and demonstrated that the mutation disrupts *innexin-16* (*inx-16*), a gene encoding a gap-junction subunit (Figure S1A in the Supplemental Data available online). Because the genes encoding invertebrate gap-junction subunits, “innexins” (invertebrate *connexins*), are now known to exist in vertebrates, the protein family has been renamed the “pannexin” family [6, 7]. Gene identity was assigned by rescue and the sequence of two *inx-16* alleles. The defects in *ox144* mutants are fully rescued by microinjection of wild-type *inx-16* (Figure S1A and Figures 1B and 3B–3E). The two alleles exhibit similar phenotypes (Figures 3B–3E); *ox144* allele is an early stop, and *tm1589* is a deletion in the 5' region of the gene (Figure S1A). RNA interference of *inx-16* resulted in defects identical to those of *ox144* (Figures 3B–3E) [8]. Because the pannexin gene *inx-17* is in an operon downstream of *inx-16*, it was possible that reducing *inx-17* expression would cause similar phenotypes to that of *inx-16* mutants. However, *inx-17* RNAi did not produce any visible phenotype. We conclude that the defects observed in the *ox144* strain are due to mutation of the pannexin gene *inx-16*.

The INX-16 Protein Is Localized to Cell-Cell Contacts in the Intestine

To determine whether *inx-16* is expressed in the intestine, the cellular location of the defecation clock, we expressed GFP under the *inx-16* promoter. This transcriptional reporter is expressed in the intestine (Figure 1A and Figures S1B–S1D). Gap-junction components from adjacent cells typically assemble into channels between the cells; however, they can also be oriented toward extracellular space and function as hemichannels [9, 10]. To determine whether INX-16 is likely to be forming gap junctions or hemichannels, we determined the subcellular location of the protein by tagging it with GFP (Figure 1B and Figure S1A). The INX-16:GFP fusion protein fully rescues the *inx-16*(*ox144*) mutant phenotypes (Figures 3B–3E), suggesting that the tagged protein is localized correctly. The *C. elegans* intestine is a tube composed of rings of paired cells [11] (Figures 1D and 1E). In electron micrographs, gap junctions can be observed in areas where intestinal cells contact one another (Figure 1C). Similarly, INX-16:GFP fluorescence is localized to the sites of cell contacts between intestinal cells but is

*Correspondence: jorgensen@biology.utah.edu

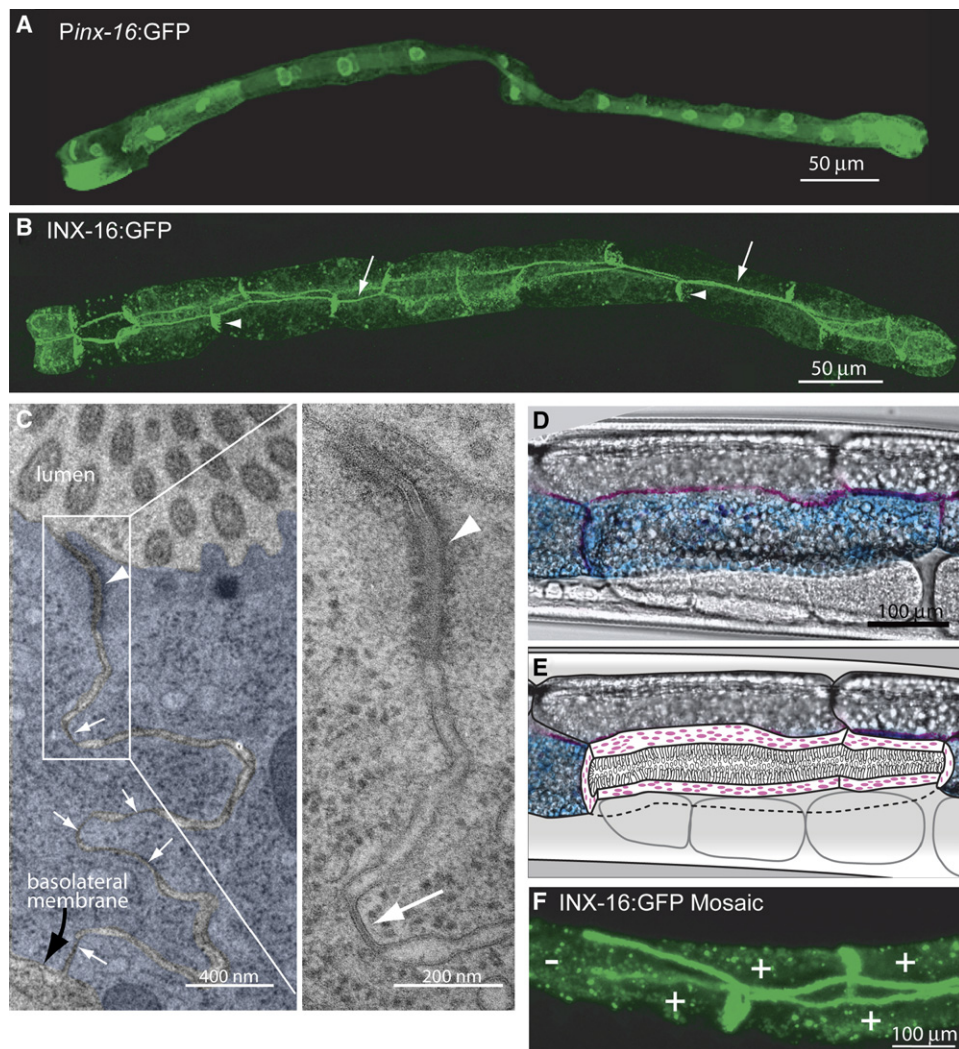


Figure 1. Expression Pattern of Pannexin *inx-16*

(A) Expression of GFP driven by the promoter of *inx-16* (plasmid pMAP4). Fluorescence is observed in the intestine of an adult worm. GFP accumulates in the nuclei (bright circles). The anterior is to the left.

(B) Expression of a functional translational fusion protein INX-16:GFP (plasmid pMAP3). The fluorescent fusion protein is localized to the sites of intestinal cell-cell contacts. The arrows mark the dorsal-ventral contacts of two intestinal cells in a ring, and the arrowheads mark the anterior-posterior sites of intestinal cell contacts.

(C) Electron micrograph of an intestinal cell-cell junction. A dorsal-ventral cross section of an adult intestine shows the ultrastructure of intestinal cell contacts. The white arrows mark the gap junctions between the cells, and the arrowhead marks the adherens junctions. The black arrow points to the basal membrane of one intestinal cell. On the right, an enlargement of the region bracketed by the white lines is shown.

(D) Double labeling of a functional translational fusion protein INX-16:GFP (plasmid pMAP3) and intestinal plasma membranes with *Pvit-2:myr-mCherry* (pJPW1). The myr-mCherry (cyan) is localized to the plasma membrane, and INX-16:GFP puncta (magenta) are present at the sites of cell-cell contact. The confocal images are superimposed on a nomarski image of the intestine. Some intestinal cells are not included in the confocal stack and therefore are not colored.

(E) Interpretative diagram of intestinal cells shown in (D). One intestinal cell has been removed from the intestinal tube so that the approximate localization of INX-16:GFP at cell junctions could be shown. The lumen is indicated by the presence of microvilli; the INX-16 puncta are shown as magenta dots. The dashed line marks the edge of the removed cell.

(F) The intestine of a mosaic animal expressing INX-16:GFP in a subset of intestinal cells. Cells expressing INX-16:GFP are marked with a "+," and cells not expressing INX-16:GFP are marked with a "-." Normal localization of INX-16:GFP was observed at cell-cell contacts between INX-16:GFP expressing cells but is absent from cell-cell contacts between expressing and nonexpressing cells.

excluded from other surfaces (Figures 1B, 1D, and 1E), consistent with localization to gap junctions.

To determine whether INX-16-containing hemichannels are interacting with subunits in adjacent cells, we analyzed mosaic animals. If the gap-junction protein is not expressed in an adjacent cell, INX-16 is not localized

to that side of the cell (Figure 1F). Connexons can form functional gap junctions by interacting with other subunits to form a junctional complex [12]. By contrast, INX-16 requires a homomeric interaction for junctional localization, despite the fact that other pannexin subunits are likely to be expressed in the gut (see below).

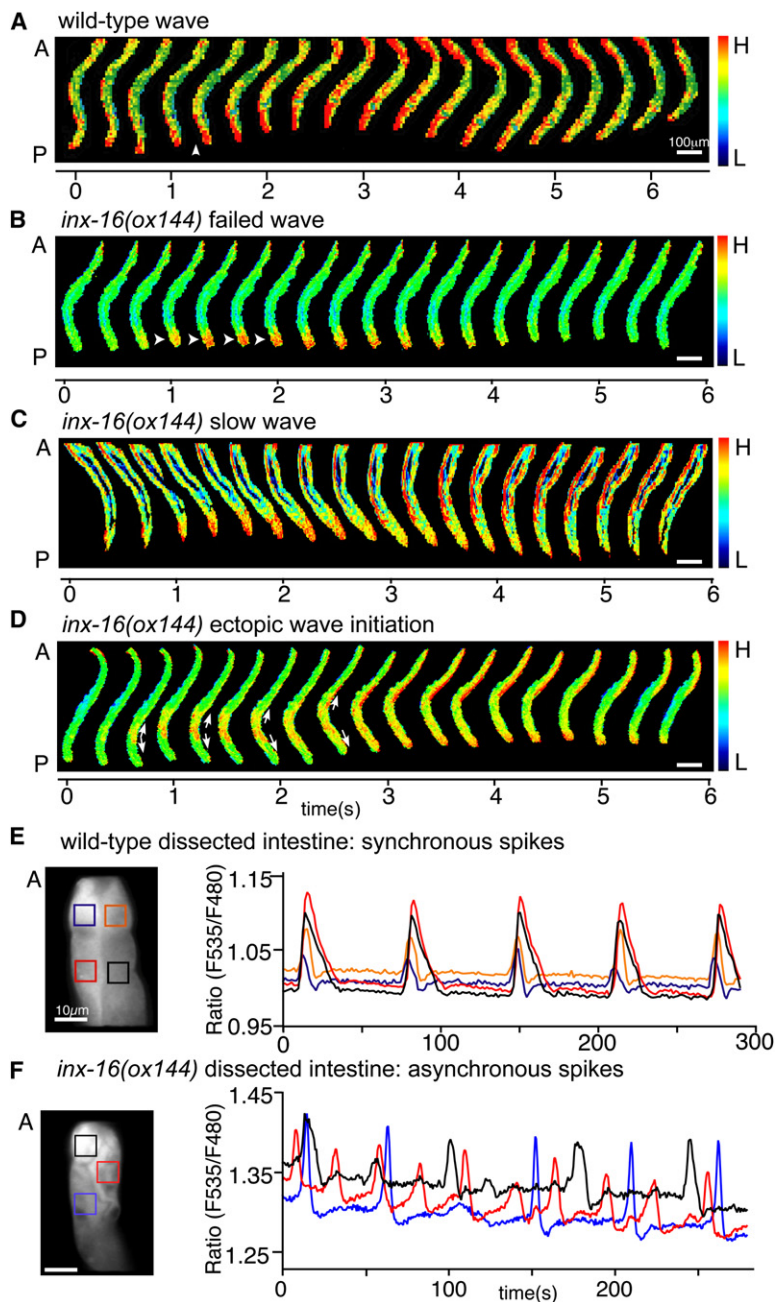


Figure 2. Intestinal Calcium Dynamics in Wild-Type and *inx-16(ox144)* Adult Animals (A–D) Representative frames of movies of calcium waves imaged with cameleon. Consecutive panels are shown. Time, in seconds, is depicted along the x axis. The anterior (A) end of the intestine is at the top of the image, and the posterior (P) end is at the bottom. In these images, fluorescence intensity (ratio 535 nm/480 nm) has been depicted with a “rainbow” lookup table. The range of the “rainbow” lookup table is shown in the bar to the right of images. A high ratio (H) indicating high calcium is coded red, whereas a low ratio (L) indicating low calcium is blue. In (A), intestinal calcium wave in an undissected wild-type worm (*tgEx83[Pgtl-1:YC2.12]*) is shown. The white arrowhead marks the initiation of the posterior body contraction. The midsection of this worm has lower baseline fluorescence. In (B)–(D), calcium imaging of *inx-16(ox144)* animals (genotype: *inx-16(ox144); tgEx83[Pgtl-1:YC2.12]*) is shown. A failed wave is shown in (B). A calcium spike occurs in the most posterior ring of cells but does not initiate a calcium wave. The arrowhead points to the calcium spike. A slow wave is shown in (C). A calcium wave is initiated in the proper location, the most posterior intestine, but its propagation is severely retarded compared to the wild-type. An ectopic wave is shown in (D). The calcium wave initiates several cells anterior to the posterior intestinal cells and spreads in both directions (arrows).

(E–F) Calcium imaging of dissected intestinal preparations. The left panel shows the portion of wild-type or *inx-16(ox144)* gut analyzed. The anterior (A) end is on the top; at the bottom is approximately the third ring of cells. Calcium oscillations were measured in the several color-coded boxes. The right graph depicts increases in calcium levels in the boxed regions over time as determined by the ratio of fluorescence emission at 535 nm relative to 480 nm. The color of each line corresponds to a colored box in the photograph. (E) shows nearly synchronous calcium spikes in adjacent cells of a wild-type dissected intestinal preparation (*tgEx83[Pgtl-1:YC2.12]*). (F) shows that calcium oscillations are asynchronous in a dissected *inx-16(ox144); tgEx83[Pgtl-1:YC2.12]* intestine.

Gap Junctions Shape the Calcium Wave

To determine whether the propagation of the calcium wave requires *inx-16*, we compared intestinal calcium dynamics of wild-type and *inx-16(ox144)* worms by using genetically encoded calcium sensors [1, 13–15]. In behaving worms, a calcium spike in the most posterior cells initiates a calcium wave that travels the length of the intestine [1] (Figure 2A). The wave travels at a speed of $340 \pm 140 \mu\text{m/s}$ ($n = 10$) and roughly matches the rate of posterior body contraction, approximately $270 \mu\text{m/s}$ [1] (Movies S1 and S3).

In *inx-16(ox144)* animals, the spatial and temporal patterns of calcium waves are altered in three ways ($n = 34$). First, the propagation of the calcium wave was

eliminated in 21% of *inx-16(ox144)* animals (7/34). In these animals, only the most posterior cells experienced a calcium spike; there was no calcium wave (Figure 2B). Second, in animals with a calcium wave, the speed of the calcium wave was retarded (Figure 2C, $n = 12$). In these animals, propagation was severely decreased and fell into two categories, 3-fold or 9-fold slower than in the wild-type (*inx-16* slow: $108 \pm 29 \mu\text{m/s}$, 4/12; *inx-16* very slow: $39 \pm 14 \mu\text{m/s}$, 8/12; wild-type: $340 \pm 140 \mu\text{m/s}$, $n = 10$) [1]. These data suggest that gap junctions are still present between intestinal cells in the mutant. To test whether there are still functional gap junctions in *inx-16* mutants, we injected the small molecule, lucifer yellow, into intestines. Dye transfer was not

qualitatively different in *inx-16* and the wild-type (data not shown), demonstrating the presence of residual gap junctions. One of the 24 other *C. elegans* pannexins may account for these residual calcium waves [6]. Third, the site of initiation was frequently aberrant in those animals with waves. In more than half of these animals, the initial calcium spike did not occur in the most posterior cells (17/27). Instead the calcium wave began in more anterior intestinal cells and spread outward in both directions (Figure 2D and Movie S2).

In dissected preparations of wild-type animals, calcium flux propagates through intestinal cells (Figure 2E) [1, 2]. However, in dissected *inx-16(ox144)* intestines, abnormal calcium dynamics are observed, demonstrating that the defects observed in *inx-16* mutants are intrinsic to the intestine. The calcium spikes occur asynchronously and appear to be independent from neighboring cells (Figure 2F), suggesting that INX-16 is required for cell-cell coupling during wave propagation.

In vertebrates, calcium waves can also be propagated indirectly by release of ATP through hemichannels that activate purinergic receptors on adjacent cells [9, 16–19]. However, the data described above demonstrate that the calcium wave in the intestine depends on gap junctions. First, INX-16 is localized to cell-cell contacts, coincident with sites of gap junctions. Second, INX-16 localization requires expression in both contacting cells. Third, calcium waves propagate in the dissected intestine, where the extracellular volume is large [1, 2]. Fourth, purinergic receptors are not present in the *C. elegans* genome.

What is the molecule that passes through the pannexin gap junction? IP₃ activates the IP₃ receptor, and it is conceivable that IP₃ passes through the junctions to initiate a calcium wave in every cell. Alternatively, calcium itself could be the signal that travels through the gap junction because calcium can produce a regenerative spike [20]. Thus, calcium flux from one cell to an adjacent cell through gap junctions could stimulate a regenerative calcium spike.

***inx-16(ox144)* Mutants Have Defective Motor Programs**

If the calcium wave is an important regulator of the defecation cycle (Figure 3A), then disrupting the calcium wave should lead to defecation cycle defects. *inx-16(ox144)* hermaphrodites were isolated because they were very constipated (Figure S2). Compared to wild-type animals, *inx-16(ox144)* animals are smaller, grow more slowly (4 versus 3 days to reach adulthood), have decreased brood size (158 ± 19 progeny, n = 4 versus 241 ± 17, n = 5), and exhibit multiple defects in the defecation cycle (see below). These phenotypes are due to a functional role of *inx-16* rather than developmental abnormalities, because the defecation-cycle defects can be rescued in the adult. Specifically, expression of *inx-16* in the adult intestine under the *vitellogenin-2* (*Pvlt-2*) promoter [21] rescues the defecation-cycle defects (Figures 3D and 3E).

A detailed analysis of the defecation cycle demonstrates that three aspects of the motor program are disrupted in these mutants: they exhibit variable cycle timing, possess abnormal posterior body contractions,

and predominantly lack the later steps of the motor program [3].

First, INX-16 gap junctions are required for reliable timing of the defecation clock. The median cycle time of wild-type worms only varies 6 s, from 43–49 s. The median cycle time for individual *inx-16(ox144)* worms varies by 28 s, from 34–62 s (Figure 3B). Individual cycles times within a single *inx-16* worm are also variable, although this phenotype differs among the genotypes (Figure 3C). These data suggest that intercellular communication mediated by gap junctions is required for consistent timing of the clock.

Second, the calcium wave is required for the normal dynamics of the posterior body contraction. In the wild-type, the wave of contraction sweeps forward from the tail, thereby causing the posterior intestine to fold up like an accordion (Figures 4A–4C and Movie S3). In mutant animals exhibiting a wave of contraction, the posterior body contractions are slower and appear saltatory rather than smooth (Figures 4D–4F). In some *inx-16(ox144)* animals, the contractions initiate midintestine and slowly move backward (Figures 4D–4G; Movies S2 and S4). Occasionally saltatory calcium wave progression is observed (Movie S1). These contraction abnormalities—reversed, slowed, or saltatory progression—match the abnormal calcium waves observed in these mutants.

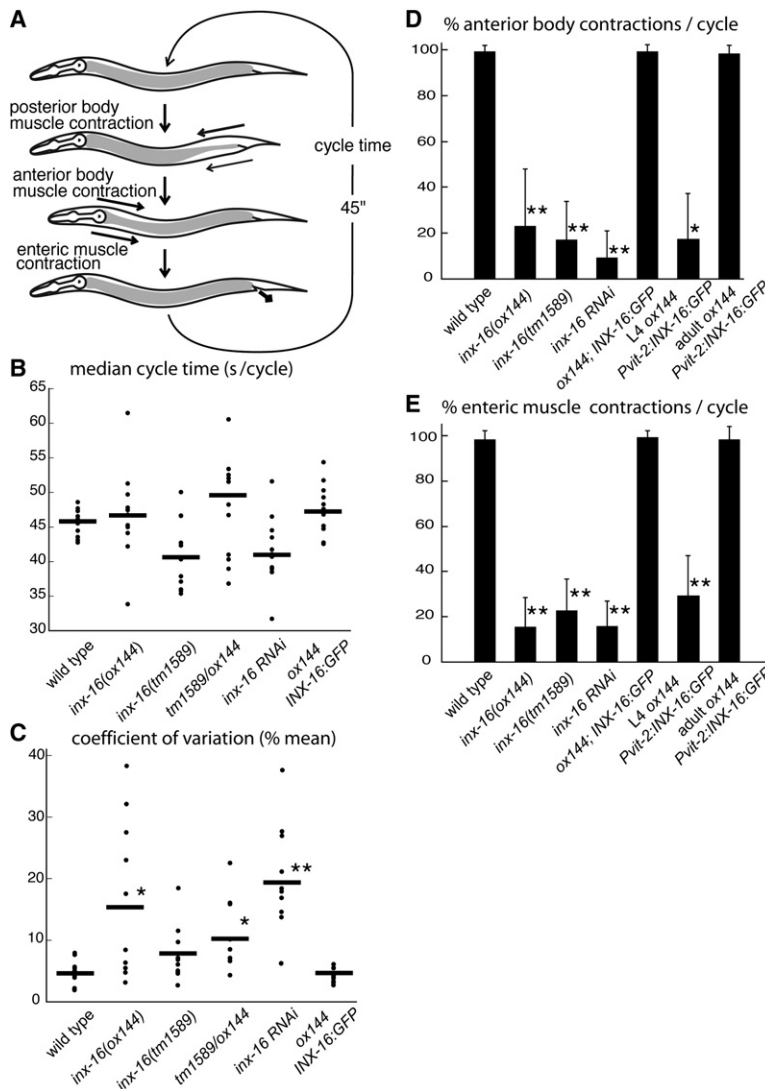
To determine whether there is a one-to-one correlation in the direction and speed of the calcium wave and the posterior body contraction, we characterized muscle contractions while simultaneously monitoring calcium waves. We observed contraction of the adjacent body muscles in register with the intestinal calcium increases (n = 4). Calcium waves that initiated in the middle of the animal and proceeded posteriorly were associated with a contraction that also initiated in the middle of the intestine and proceeded posteriorly (Figure 4G and Movie S2). These data suggest that the intestinal calcium wave instructs contraction of the overlying muscle during the posterior body contraction.

Third, the last two contractions, the anterior body-muscle and enteric-muscle contractions, are usually absent in *inx-16* mutants. Wild-type worms almost always execute both of these motor steps. *inx-16(ox144)* adults execute an anterior body contraction in only 24% of the defecation cycles and execute an enteric-muscle contraction in only 16% of the defecation cycles (Figures 3D and 3E). Again, the presence of these muscle contractions varies between individual worms (see error bars, Figures 3D and 3E). Calcium flux in the anterior intestine is required for the anterior and enteric-muscle contractions [1]; thus, the failure of calcium waves to properly propagate into the anterior cells is likely to be responsible for this phenotype.

These findings lead to two important insights into defecation-cycle signaling. First, gap junctions maintain the supremacy of the pacemaker cell and the precision of the clock. Second, the spatiotemporal pattern of the wave controls signaling downstream of the clock.

Gap Junctions Maintain the Supremacy and Reliability of Pacemaker Activity

Who is the timekeeper? In wild-type animals, the posterior ring of cells initiate the calcium wave. However,



17.3% ± 16.8%; *inx-16* RNAi: 11.9% ± 14.0%, *inx-16(ox144) oxEx524[INX-16:GFP]*: 99.1% ± 3.0%; L4 (larval stage 4) *inx-16(ox144) oxEx557[Pvit-2:INX-16:GFP]*: 17.3% ± 20.0%; adult *inx-16(ox144) oxEx557[Pvit-2:INX-16:GFP]*: 98.2% ± 6.0%. **p* < 0.05 and ***p* < 0.0005 with an unpaired Student's *t* test with unequal variance.

(E) Percentage of enteric-muscle contraction per cycle. The mean percentage of enteric-muscle contractions per cycle is shown; ten motor programs are scored per worm (mean ± SD, wild-type: 98.2% ± 4.0%; *inx-16(ox144)* 15.5% ± 12.9%; *inx-16(tm1589)*: 22.7% ± 14.2%; *inx-16* RNAi: 15.6% ± 11.3%; *inx-16(ox144) oxEx524[INX-16:GFP]*: 99.1% ± 3.0%; L4 (larval stage 4) *inx-16(ox144) oxEx557[Pvit-2:INX-16:GFP]*: 29.1% ± 18.7%; adult *inx-16(ox144) oxEx557[Pvit-2:INX-16:GFP]*: 98.2% ± 6.0%). ***p* < 0.0005 with an unpaired Student's *t* test with unequal variance.

greater than half of the *inx-16* mutant calcium waves initiated in an ectopic cell. These data suggest that the most posterior cell is not fundamentally different from all other intestinal cells; other intestinal cells are capable of initiating a calcium wave in the absence of the normal pacemaker. Like in the vertebrate heart, worm intestinal pacemaker function might simply be conferred on the first cell that produces a calcium spike; intercellular coupling then might force all secondary pacemakers to fire simultaneously.

How does the pacemaker keep time? Previous data indicated that the precise timing of the cycle is controlled at least in part by IP₃ levels [2, 4, 22, 23]. However, the reliability of the pacemaker also depends on *inx-16* function. Cycle periodicity is more erratic in *inx-16(ox144)* animals compared to the wild-type. Although

Figure 3. Characterization of *inx-16(ox144)* Motor-Program Defects

(A) The defecation cycle in *C. elegans*. Worms execute the motor program approximately every 45–50 s. During the posterior body-muscle contraction, the body muscles surrounding the intestine contract as an anteriorly directed wave, forcing contents of the gut forward. Approximately 3 or 4 s later, the anterior body muscles contract, thereby forcing the contents of the gut backward. This is followed a 1/2 s later by enteric-muscle contraction, which opens the anus and forcibly expels the contents of the gut. (B) Defecation-cycle period. The median cycle time for each worm scored is denoted by a dot. Cycle time is defined as the average time between posterior body contractions for ten defecation cycles. The horizontal bar marks the average median of 11 worms for each genotype (wild-type: 45.60 s; *inx-16(ox144)*: 46.82 s; *inx-16(tm1589)*: 41.00 s, *p* < 0.05; *inx-16(ox144) dpy-5(e61)/inx-16(tm1589)*: 49.03 s; *inx-16* RNAi: 41.65 s, *p* < 0.05; *inx-16(ox144); oxEx524 [INX-16:GFP]*: 47.61 s); *p* values were calculated with an unpaired Student's *t* test with unequal variance.

(C) Variation of cycle time. The coefficient of variation for each worm scored is denoted by a dot. The horizontal bar marks the mean coefficient of variation of 11 worms for each genotype (mean ± SD, wild-type: 4.9 ± 1.9; *inx-16(ox144)*: 15.7 ± 12.7, *p* < 0.05; *inx-16(tm1589)*: 7.9 ± 4.3, *p* = 0.055; *inx-16(ox144)dpy-5(e61)/inx-16(tm1589)*: 10.3 ± 5.5, *p* < 0.05; *inx-16* RNAi: 19.1 ± 9.3, *p* < 0.0005; *inx-16(ox144); oxEx524 [INX-16:GFP]*: 4.5 ± 1.1). **p* < 0.05 and ***p* < 0.0005 with an unpaired Student's *t* test with unequal variance.

(D) Percentage of anterior body contraction per cycle. The mean percentage of anterior body contractions per cycle is shown; ten motor programs are scored per worm (mean ± SD, wild-type: 99.1% ± 3.0%; *inx-16(ox144)*: 23.6% ± 24.6%; *inx-16(tm1589)*: 19.1% ± 14.2%; *inx-16* RNAi: 15.6% ± 11.3%; *inx-16(ox144) oxEx524[INX-16:GFP]*: 99.1% ± 3.0%; L4 (larval stage 4) *inx-16(ox144) oxEx557[Pvit-2:INX-16:GFP]*: 29.1% ± 18.7%; adult *inx-16(ox144) oxEx557[Pvit-2:INX-16:GFP]*: 98.2% ± 6.0%). **p* < 0.05 and ***p* < 0.0005 with an unpaired Student's *t* test with unequal variance.

the calcium wave is likely to synchronize the activity of adjacent intestinal cells, the erratic periodicity suggests that gap-junction communication also serves to reinforce the timekeeper.

Calcium-Wave Pattern Controls Downstream Signaling Events

In most systems, the calcium wave is the main event; in the heart, it directly causes muscle contraction. By contrast, in *C. elegans* the calcium wave is instructive for events in other tissues, specifically the contraction of posterior body muscles and the activation of motor neurons innervating the enteric muscles. Posterior body contractions directly obey the dynamics of the calcium wave. First, there is slowing of the calcium wave and posterior-body-contraction progression in *inx-16*

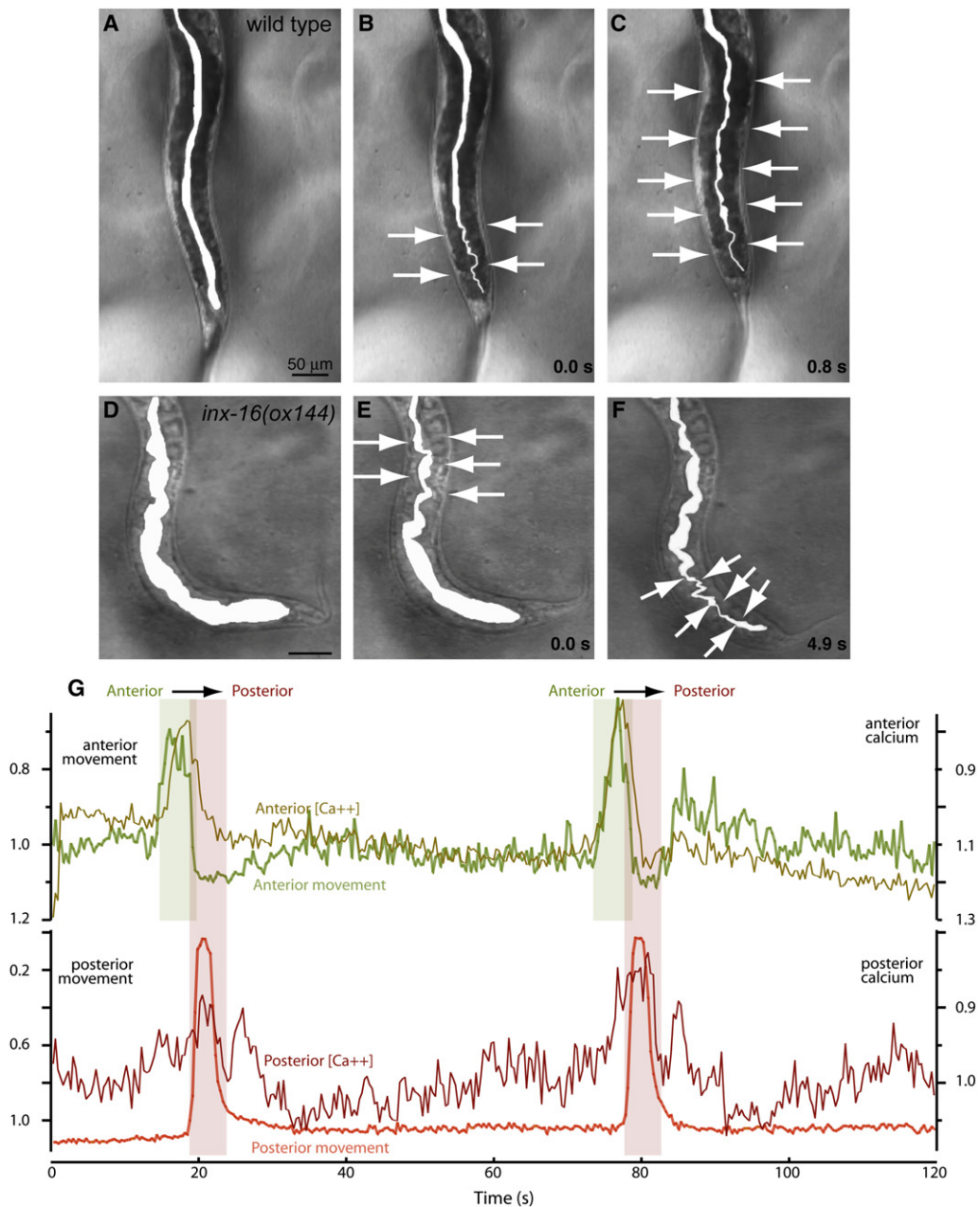


Figure 4. Posterior Body Contraction Occurs Point-by-Point from Intestine to Body Wall Muscle

(A–C) The lumen of a wild-type worm is shaded in white. (A) shows the worm just prior to contraction. The arrows mark the region of contraction. The time relative to the beginning of posterior body contraction is marked on the lower right in seconds.

(D–F) The lumen of an *inx-16(ox144)* worm is shaded in white. (D) shows the worm just prior to contraction. In (E) and (F), arrows mark the area of contraction. In (F), the region contracted in (E) has already begun to relax because of the lengthened posterior body contraction period.

(G) Calcium flux and movement measurements. In this animal, a slow calcium wave initiated in an anterior intestinal cell and proceeded posteriorly. Calcium changes were measured with inverse pericam in two regions of the intestine, one anterior and another posterior. The top panel shows the anterior region of interest, and the bottom panel shows the posterior region of interest. The calcium imaging system does not allow visualization of the body wall muscles, but contraction of the overlying body muscle causes the intestine to be compressed, resulting in a decrease in intestinal area. Movement is represented by the lighter hues and is a measure of the change in intestinal area in the region of interest. The change in area was normalized and inverted. The darker lines are the change in fluorescence intensity. The measurements are normalized and inverted because inverse-pericam fluorescence decreases in responses to increases in calcium concentration. The period of calcium flux and contraction in the anterior region of interest is enclosed in a light-green box and the period of calcium flux, and contraction in the posterior region of interest is enclosed in a light-red box.

mutants. Second, there was a direct correlation of backward calcium waves and backward muscle contractions. Third, saltatory calcium spikes in intestinal cells were associated with focal contractions in adjacent

muscles. These data suggest that a signal is transmitted from an intestinal cell to a muscle cell in a point-to-point fashion. Point-to-point signaling is surprising because body muscles are connected by gap junctions [24–26].

These data suggest a calcium increase in one intestinal ring leads to the contraction of the muscle overlying that ring. The smooth contraction of the body muscles is coordinated by the intestinal calcium wave, rather than by gap junctions in the muscles. Thus, there must be a calcium-sensitive release of transmitter from the intestine onto the overlying body muscles during the posterior body contraction.

Loss of INX-16 almost completely eliminates the late motor steps, anterior and enteric-muscle contractions. Again, the intestinal calcium wave is likely to stimulate the release of a transmitter that activates the motor neurons responsible for these behaviors [27]. These contractions require certain proteins, such as AEX-1 and AEX-6/Rab27, that are expressed in the intestine [28, 29]. These proteins might mediate secretion of transmitter from the intestine in response to the calcium wave.

In addition to these direct effects on the defecation motor program, INX-16-mediated calcium waves may have broad effects on neuronal function. *inx-16* mutants are resistant to the paralyzing effects of the acetylcholinesterase inhibitor aldicarb (Figure S3). Because *inx-16* is only expressed in the intestine, a paracrine signal may modulate output from acetylcholine motor neurons. Thus, the intestine may function as an endocrine organ to control multiple tissues, as well as to coordinate different components of a behavioral program.

Supplemental Data

Experimental Procedures, three figures, and four movies are available at <http://www.current-biology.com/cgi/content/full/17/18/1601/DC1/>.

Acknowledgments

We thank Paola Dal Santo Nix and Matthew Miller for initial mapping experiments, Jim Lechleiter for inverse pericam and helpful advice, Nels Jorgensen for electron microscopy, Glen Ernstrom for imaging assistance, Ewa Bednarek for statistical advice, M. Wayne Davis for critical readings of this manuscript, and all Jorgensen laboratory members for helpful suggestions. The allele *tm1589* was isolated by the National Bioresource Project for the Experimental Animal "Nematode *C. elegans*" in Japan. A. Coulson and the Sanger Center provided cosmid clones. Some strains used in this work were provided by the *Caenorhabditis* Genetics Center, which is funded by the National Institutes of Health (NIH) National Center for Research Resources (NCR). This work was supported by a NIH Grant MH60997 (E.M.J.), a NIH NRSA GM64222-01 (M.A.P.), and Northwestern University Funds (K.I.). K.I. is a Kyakuin-Kenkyuin Scientist of the Agency of Industrial Science and Technology in Japan. E.M.J. is an Investigator of the Howard Hughes Medical Institute. Correspondence and request for materials should be addressed to jorgensen@biology.utah.edu.

Received: January 31, 2007

Revised: August 7, 2007

Accepted: August 8, 2007

Published online: September 6, 2007

References

1. Teramoto, T., and Iwasaki, K. (2006). Intestinal calcium waves coordinate a behavioral motor program in *C. elegans*. *Cell Calcium* 40, 319–327.
2. Espelt, M.V., Estevez, A.Y., Yin, X., and Strange, K. (2005). Oscillatory Ca²⁺ signaling in the isolated *Caenorhabditis elegans* intestine: Role of the inositol-1,4,5-trisphosphate receptor and phospholipases C beta and gamma. *J. Gen. Physiol.* 126, 379–392.
3. Thomas, J.H. (1990). Genetic analysis of defecation in *Caenorhabditis elegans*. *Genetics* 124, 855–872.
4. Branicky, R., and Hekimi, S. (2006). What keeps *C. elegans* regular: The genetics of defecation. *Trends Genet.* 22, 571–579.
5. Dal Santo, P., Logan, M.A., Chisholm, A.D., and Jorgensen, E.M. (1999). The inositol trisphosphate receptor regulates a 50-second behavioral rhythm in *C. elegans*. *Cell* 98, 757–767.
6. Phelan, P., and Starich, T.A. (2001). Innexins get into the gap. *Bioessays* 23, 388–396.
7. Panchin, Y., Kelmanson, I., Matz, M., Lukyanov, K., Usman, N., and Lukyanov, S. (2000). A ubiquitous family of putative gap junction molecules. *Curr. Biol.* 10, R473–R474.
8. Kamath, R.S., and Ahringer, J. (2003). Genome-wide RNAi screening in *Caenorhabditis elegans*. *Methods* 30, 313–321.
9. Goodenough, D.A., and Paul, D.L. (2003). Beyond the gap: Functions of unpaired connexon channels. *Nat. Rev. Mol. Cell Biol.* 4, 285–294.
10. Barbe, M.T., Monyer, H., and Bruzzone, R. (2006). Cell-cell communication beyond connexins: The pannexin channels. *Physiology (Bethesda)* 21, 103–114.
11. Sulston, J.E., Schierenberg, E., White, J.G., and Thomson, J.N. (1983). The embryonic cell lineage of the nematode *Caenorhabditis elegans*. *Dev. Biol.* 100, 64–119.
12. Swenson, K.I., Jordan, J.R., Beyer, E.C., and Paul, D.L. (1989). Formation of gap junctions by expression of connexins in *Xenopus* oocyte pairs. *Cell* 57, 145–155.
13. Nagai, T., Sawano, A., Park, E.S., and Miyawaki, A. (2001). Circularly permuted green fluorescent proteins engineered to sense Ca²⁺. *Proc. Natl. Acad. Sci. USA* 98, 3197–3202.
14. Miyawaki, A., Griesbeck, O., Heim, R., and Tsien, R.Y. (1999). Dynamic and quantitative Ca²⁺ measurements using improved cameleons. *Proc. Natl. Acad. Sci. USA* 96, 2135–2140.
15. Miyawaki, A., Llopis, J., Heim, R., McCaffery, J.M., Adams, J.A., Ikura, M., and Tsien, R.Y. (1997). Fluorescent indicators for Ca²⁺ based on green fluorescent proteins and calmodulin. *Nature* 388, 882–887.
16. Bruzzone, R., Hormuzdi, S.G., Barbe, M.T., Herb, A., and Monyer, H. (2003). Pannexins, a family of gap junction proteins expressed in brain. *Proc. Natl. Acad. Sci. USA* 100, 13644–13649.
17. Bao, L., Locovei, S., and Dahl, G. (2004). Pannexin membrane channels are mechanosensitive conduits for ATP. *FEBS Lett.* 572, 65–68.
18. Locovei, S., Wang, J., and Dahl, G. (2006). Activation of pannexin 1 channels by ATP through P2Y receptors and by cytoplasmic calcium. *FEBS Lett.* 580, 239–244.
19. Vanden Abeele, F., Bidaux, G., Gordienko, D., Beck, B., Panchin, Y.V., Baranova, A.V., Ivanov, D.V., Skryma, R., and Prevarskaya, N. (2006). Functional implications of calcium permeability of the channel formed by pannexin 1. *J. Cell Biol.* 174, 535–546.
20. Bezprozvanny, I., Watras, J., and Ehrlich, B.E. (1991). Bell-shaped calcium-response curves of Ins(1,4,5)P₃- and calcium-gated channels from endoplasmic reticulum of cerebellum. *Nature* 351, 751–754.
21. MacMorris, M., Broverman, S., Greenspoon, S., Lea, K., Madej, C., Blumenthal, T., and Spieth, J. (1992). Regulation of vitellogenin gene expression in transgenic *Caenorhabditis elegans*: Short sequences required for activation of the *vit-2* promoter. *Mol. Cell Biol.* 12, 1652–1662.
22. Walker, D.S., Gower, N.J., Ly, S., Bradley, G.L., and Baylis, H.A. (2002). Regulated disruption of inositol 1,4,5-trisphosphate signaling in *Caenorhabditis elegans* reveals new functions in feeding and embryogenesis. *Mol. Biol. Cell* 13, 1329–1337.
23. Norman, K.R., Fazio, R.T., Mellem, J.E., Espelt, M.V., Strange, K., Beckerle, M.C., and Maricq, A.V. (2005). The Rho/Rac-family guanine nucleotide exchange factor VAV-1 regulates rhythmic behaviors in *C. elegans*. *Cell* 123, 119–132.
24. Liu, Q., Chen, B., Gaier, E., Joshi, J., and Wang, Z.W. (2006). Low conductance gap junctions mediate specific electrical coupling in body-wall muscle cells of *Caenorhabditis elegans*. *J. Biol. Chem.* 281, 7881–7889.

25. White, J.G., Southgate, E., Thomson, J.N., and Brenner, S. (1976). The structure of the ventral nerve cord of *Caenorhabditis elegans*. *Philos. Trans. R. Soc. Lond. B Biol. Sci.* 275, 327–348.
26. Hall, D.H., Lints, R., and Altun, Z. (2005). Nematode neurons: Anatomy and anatomical methods in *Caenorhabditis elegans*. *Int. Rev. Neurobiol.* 69, 1–35.
27. McIntire, S.L., Jorgensen, E., Kaplan, J., and Horvitz, H.R. (1993). The GABAergic nervous system of *Caenorhabditis elegans*. *Nature* 364, 337–341.
28. Doi, M., and Iwasaki, K. (2002). Regulation of retrograde signaling at neuromuscular junctions by the novel C2 domain protein AEX-1. *Neuron* 33, 249–259.
29. Mahoney, T.R., Liu, Q., Itoh, T., Luo, S., Hadwiger, G., Vincent, R., Wang, Z.W., Fukuda, M., and Nonet, M.L. (2006). Regulation of synaptic transmission by RAB-3 and RAB-27 in *Caenorhabditis elegans*. *Mol. Biol. Cell* 17, 2617–2625.

A Calcium Wave Mediated by Gap Junctions Coordinates a Rhythmic Behavior in *C. elegans*

Maureen A. Peters, Takayuki Teramoto,
Jamie Q. White, Kouichi Iwasaki
and Erik M. Jorgensen

Supplemental Experimental Procedures

Strains

Nematodes were cultured in accordance with standard methods [S1]. The wild-type is the N2 isolate from Bristol, England. *inx-16* mutant strains are EG144 *inx-16(ox144)* I and EG3528 *inx-16(tm1589)* I. Information about the *ox144* allele has been submitted to Wormbase (www.wormbase.org). *tm1589* was isolated by the National Bioresource Project for the Experimental Animal *C. elegans* and is also described on Wormbase. We generated EG3528 by outcrossing FX1589 *inx-16(tm1589)* four times. *inx-16* expression analysis was done with strain EG3264 *oxEx558[Pinx-16:GFP]* and EG3233 *oxls143[INX-16:GFP; lin-15(+)] V; lin-15(n765ts) X*. A strain containing myristylated mCherry (*myr-mCherry*) under the control of an adult intestine promoter, and INX-16:GFP, was created so that INX-16:GFP's subcellular localization (EG4729 *him-5(e1490) V; lin-15(n765ts) X; oxEx1042[Pvit-2:myr-mCherry; INX-16:GFP; lin-15(+)]*) could be refined. The following strains were used for behavioral assays: EG3149 *inx-16(ox144); oxEx524[INX-16:GFP]*, EG3256 *inx-16(ox144); oxEx557[Pvit-2:INX-16(cDNA):GFP; Pmyo-2:GFP]*, GR1373 *eri-1(mg366) IV*, and EG1772 *inx-16(ox144) dpy-5(e61) I*. For inverse-pericam imaging, strains EG3092 *lin-15(n765ts); oxEx504[Pges-1:INVERSE-PERICAM; lin-15(+)]* and EG3093 *inx-16(ox144); oxEx504[Pges-1:INVERSE-PERICAM; lin-15(+)]* were used. For cameleon imaging, KY5340 *lin-15(n765ts); tgEx83[Pgtl-1:YC2.12, lin-15(+)]* and KY5476 *inx-16(ox144); tgEx83[Pgtl-1:YC2.12; lin-15(+)]* were used.

Behavioral Assays

A defecation cycle consists of a posterior body contraction, followed by an anterior body contraction and an enteric-muscle contraction [S2]. Actively feeding first- or second-day adults were assayed at room temperature (22°C) for ten motor programs. Eleven animals were scored for all genotypes. The coefficient of variation listed is the percent mean of each animal's coefficient of variation (SD/mean) × 100. Statistical significance was calculated with unpaired Student's *t* tests, with unequal variance.

Rescuing Constructs

Transgenic-array strains were generated by standard microinjection techniques. We obtained cosmid rescue by injecting 20 ng/μl cosmid R12E2, 10 ng/μl *Punc-122:GFP* [coelomocyte:GFP] [S3], and 100 ng/μl DNA ladder to generate the extrachromosomal array. We created the genomic rescuing array *oxEx486* by injecting 4 ng/μl of a PCR product containing the *inx-16* and *inx-17* ORFs (plus 284 bp *inx-16* 5' upstream sequence), 10 ng/μl *Punc-122:GFP*, and 70 ng/μl DNA ladder. Three strains containing *oxEx486* were created: EG3063, EG3064 and EG3074.

GFP Constructs

Transcriptional Reporters

pMAP1 was created by amplification of 284 bp 5' of the *inx-16* start codon with primers that added a 5' SphI site and a 3' AgeI site. The fragment was then cloned into the SphI-AgeI sites of the Fire vector p95.75, which contains GFP coding sequence upstream of the *unc-54* 3' UTR. pMAP1 does not contain the two GATA boxes upstream of *inx-16* and is expressed in the intestine, the pharynx, and the rectal valve cell. The *inx-16* translational reporter INX-16:GFP (pMAP3, described below) contained 830 bp 5' upstream sequence and was expressed exclusively in the intestine. To reconcile the two different expression patterns, we created pMAP4 from pMAP1 and pMAP3. A SacI (blunted)-KpnI fragment from pMAP3 was ligated into pMAP1 cut with SphI (blunted) and KpnI. pMAP4 contains 830 bp 5' upstream *inx-16* start and includes essentially the entire

shared promoter region of *inx-16* and the divergently transcribed *inx-15*. This region includes the two GATA boxes and is expressed exclusively in the intestine. The *inx-16* transcriptional reporter strains were created by injection of 5 ng/μl of pMAP4 [*Pinx-16:GFP*] and 96 ng/μl of DNA ladder into the wild-type. The three independent transgenic arrays, *oxEx558*, *oxEx559*, and *oxEx560*, exhibited identical expression patterns (EG3264, EG3265, and EG3266, respectively). Images of EG3264, *oxEx558* are shown.

Translational Reporter

The INX-16:GFP construct, pMAP3, was created as follows: An *inx-16* genomic fragment containing 830 bp of 5' upstream regulatory sequence, all introns, and the 3' region was obtained by amplification of genomic DNA with primers that added a 5' SacI site and a 3' NcoI site. These sites were used for cloning the fragment into pGEM-T. Sequencing ensured an error-free open reading frame. GFP was amplified from the Fire vector, pPD95.75, with primers that added a 5' SpeI site and a 3' XbaI site. This fragment was inserted into the unique SpeI site of *inx-16* three amino acids before the carboxy terminus. This translational INX-16:GFP construct was injected into *inx-16(ox144)* worms in the following injection mix: 5 ng/μl pMAP3 and 84 ng/μl of DNA ladder for creating *oxEx524* (EG3149) and *oxEx525* (EG3150). Integrated lines (*oxls143-oxls147*) were created by injection of 5 ng/μl pMAP3, 20 ng/μl genomic *lin-15*, and 51 ng/μl 1 kb DNA ladder into *lin-15(n765ts) X* worms and subsequent X-ray integration (EG3233-EG3236).

Intestinal Expression

The *Pvit-2:INX-16(cDNA):GFP* construct, pMAP5, was created as follows: The *vitellogenin-2 (vit-2)* minimal promoter fragment was amplified with primers that added a 5' Sall site and a 3' NcoI site [S4]. An error-free *inx-16* cDNA was created by RT-PCR. Primers added a 5' AflIII site and a 3' SpeI site to the *inx-16* cDNA. A pGEM-T vector containing GFP was created by amplification of GFP from pPD95.75 with primers that added a 5' SpeI site and a 3' XbaI site. The *vit-2* and *inx-16* cDNA fragments were simultaneously cloned into the Sall-and-SpeI-cut pGEM-T:GFP vector. A Sall-NcoI fragment containing *Pvit-2:INX-16(cDNA)* was cloned into pPD95.75 (Fire vector kit), completing pMAP5 construction. *inx-16(ox144)* was injected with 10 ng/μl pMAP5 (*Pvit-2:INX-16(cDNA):GFP*), 2 ng/μl *Pmyo-2:GFP*, and 88 ng/μl DNA ladder for creating the transgenic array, *oxEx557*, EG3259. *oxEx557* was crossed into *inx-16(ox144)* for creating EG3256.

The intestine-specific inverse-pericam construct, *Pges-1:INVERSE-PERICAM*, pMAP2, was made as follows: A SpeI-blunt fragment containing ~3.5 kb of the gut esterase, *ges-1*, promoter was inserted into XbaI SmaI-cut Fire lab vector, pPD49.26. A short synthetic worm intron was inserted into the HpaI site of an inverse pericam (kindly provided by J. Lechleiter, University of Texas Health Science Center at San Antonio). The inverse-pericam sequence (with inserted intron) was cloned into the NheI NcoI sites of pPD49.26. To create the extrachromosomal array, *oxEx504*, we injected a mix containing 20 ng/μl pMAP2, 20 ng/μl *lin-15* genomic, and 80 ng/μl 1 kb DNA ladder into *lin-15(n765ts) X* to create EG3092. EG3093 was generated by crossing *oxEx504* into *inx-16(ox144)* I. The intestine cameleon construct *tgEx83* was made by injection of 100 ng/μl *Pgtl-1:YC2.12* and 50 ng/μl pLH98(*lin-15+*) into *lin-15(n765ts) X*.

The intestine-specific myristylated-mCherry construct, *Pvit-2:myr-mCherry*, pJPW1, was made as follows: A 250 bp PCR fragment with the *vit-2* promoter was generated and cloned into the Multisite Gateway donor vector pDONR-P4-P1R with the BP reaction (Invitrogen). The myristylation signal GSCIGK [S5] was next added to an mCherry containing worm introns (*myr-mCherry*) with PCR primers that added Ascl and FseI restriction sites. After digestion with Ascl and FseI, *myr-mCherry* was cloned into an Ascl-FseI cut Multisite Gateway 1-2 Entry vector containing an artificial intron sequence

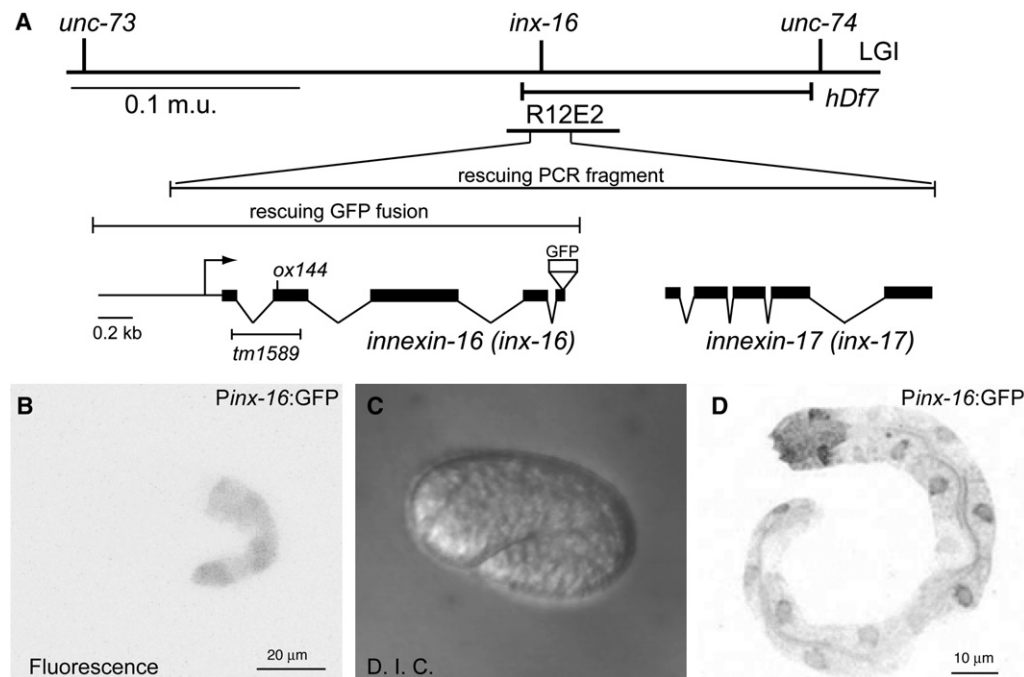


Figure S1. Genomic Structure and Developmental Expression Pattern of *inx-16*

(A) The *inx-16* locus. The top portion shows the location of *inx-16* on chromosome I. The deficiency (Df) used for mapping and the rescuing cosmid are shown below the chromosome. The extent of the PCR rescuing fragment, containing both *inx-16* and *inx-17*, is depicted above the genomic structure of the loci. *inx-17* is downstream of *inx-16* in an operon. The insertion site of green fluorescent protein (GFP) in the INX-16:GFP rescuing fusion construct is denoted. Mutations in the *inx-16* alleles are also shown. *ox144* is a C-to-T transition that results in an early stop after amino acid 104 of 372 predicted residues. *tm1589* deletes 470 base pairs of *inx-16* genomic DNA including most of exons I and II and the intervening intron (National Bioresource Project for the Experimental Animal Nematode *C. elegans*).

(B–D) Expression of GFP driven by the *inx-16* promoter (plasmid pMAP4). Fluorescence is observed in the intestine from early developmental stages. All fluorescent figures have been inverted so that fluorescence appears as black on white. In (B), GFP is observed in the intestine of a comma stage embryo. In (C) is a DIC image of embryo shown in (B). In (D), GFP is observed in the intestine of an L1 stage larva.

upstream of the mCherry. The final expression construct, pJPW1, was generated with an LR reaction with the *vit-2* promoter 4-1 Entry vector, the myristylated mCherry 1-2 Entry vector, a 2-3 Entry vector containing a generic 3' UTR from the *unc-54* gene, and the Multisite Gateway vector pDEST-R4-R3 (Invitrogen). To create the extrachromosomal array, *oxEx1042*, we injected a mix containing 20 ng/ μ l Pvit-2:myr-mCherry, 10 ng/ μ l pMAP3 (INX-16:GFP), 10 ng/ μ l *lin-15* genomic, and 60 ng/ μ l DNA ladder into the strain EG3537 *him-15(e1490); lin-15(n765ts)* X to create EG4729.

All DNA constructs, including digital ApE maps, and strains are available from the Jorgensen laboratory upon request.

Standard Microscopy

Fluorescence images of worms expressing *Pinx-16:GFP*, INX-16:GFP, Pvit-2:INX-16(cDNA):GFP, Pvit-2:myr:mCherry, and combinations therein were obtained with a Zeiss LSM5 Pascal confocal with a total magnification of 200 \times –400 \times .

Defecation cycles of wild-type and *inx-16(ox144)* animals on worm plates were digitally recorded with a Zeiss MZ12.5 stereomicroscope equipped with a digital camera. Individual frames were removed from movies with ImageJ software.

Electron Microscopy

Adult nematodes were prepared for transmission electron microscopy as previously described [S6]. Animals were placed into a freeze chamber filled with bacteria and frozen instantaneously in a high-pressure freezer (BAL-TEC HPM 010, Liechtenstein). The frozen animals were fixed in an automatic freeze substitution apparatus (Leica) with 1% osmium tetroxide and 0.1% uranyl acetate in anhydrous acetone for 2 days at -90°C ; this temperature was raised $6^{\circ}\text{C}/\text{hr}$ to -20°C over 11.7 hr, sustained at -20°C for 16 hr, and raised $10^{\circ}\text{C}/\text{hr}$ to 4°C over 4 hr. Acetone was then replaced with araldite (30% araldite for 4 hr, 70% araldite for 5 hr, 90% araldite overnight,

and pure araldite for 8 hr). Ultrathin sections (33 nm) were collected with an Ultracut E microtome. Images were obtained on a Hitachi H-7100 electron microscope with a Gatan slow-scan digital camera.

RNA Interference

RNA-mediated interference (RNAi) was performed in an *eri-1* (enhanced RNA interference) mutant background, strain GR1373 [S7]. RNAi was induced by feeding Po worms bacteria expressing double-stranded RNA targeting *inx-16* and *inx-17* (R12E.4 and R12E.5) from the Ahringer RNA library [S8]. Constipated F1 worms were selected and passaged, and constipated F2 worms were scored. The constipated phenotype was observed in $\sim 50\%$ – 90% of F2 worms. Pilot RNAi attempts in the wild-type did not yield visibly constipated worms.

Calcium Imaging and Analysis

Inverse Pericam

Young wild-type and *inx-144(ox144)* adult animals expressing inverse pericam, strains EG3092 and EG3093, respectively, were mounted and immobilized on 2% agarose pads and given food. Feeding and defecating worms were imaged at 200 \times magnification with a Biorad confocal for one to four defecation cycles at two to three frames per second. The worms were exposed to a 488 nm excitation laser, and emission was detected through a HQ 528/50 collection filter. This acquisition rate was sufficient for determining the rate of *inx-16(ox144)* waves but was too slow for determining the rate of wild-type calcium waves. To more accurately determine wave speeds, we also used cameleon imaging.

Cameleon

Wild-type and *inx-16(ox144)* animals containing an extrachromosomal array with cameleon (YC2.12) under the control of an intestine-specific promoter, *gtl-1*, were created. Strains KY5340 is *lin-15(n765ts)* X; *tgEx83[Pgtl-1:YC2.12; lin-15+]*, and KY5476 is

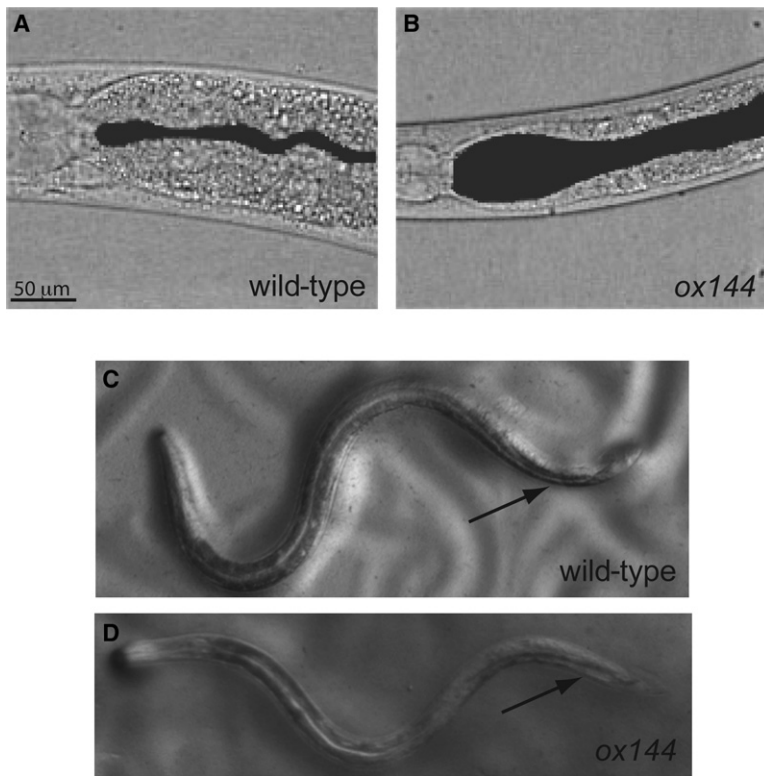


Figure S2. Comparison of Wild-Type and *inx-16(ox144)* Worms

(A and B) *inx-16(ox144)* hermaphrodites are constipated. The lumen of wild-type (A) and *ox144* intestines (B) have been colored black so that the constipated phenotype could be highlighted. The lumen of the *ox144* intestine is distended, indicating a defect in the defecation cycle. The anterior is to the left; the posterior bulb of the pharynx is visible in these adult animals.

(C and D) *inx-16(ox144)* males are constipated. The lumen of the adult *inx-16(ox144)* males (D) is distended in comparison to a wild-type male (C). The arrow marks the posterior intestine where the difference in intestinal lumen size is most striking. The anterior is to the left in these one-day adult animals.

inx-16(ox144) | *tgEx83*. For nondissected imaging, animals were put onto a 2% agarose pad, covered with a coverslip, and mounted on a fluorescence microscope. For dissected intestine preparations, animals were decapitated and imaged in the following I-T (Iwasaki-Teramoto) solution: 136 mM NaCl, 9 mM KCl, 1 mM CaCl₂, 3 mM MgCl₂, 77 mM glucose, and 5 mM HEPES (pH 7.4).

High-speed time-lapse fluorescent images of cameleon expressing worms were acquired with the AQUACOSMOS software with a W-View beam splitter and HiSCA CCD camera (Hamamatsu Photonics) optical system. The images were captured 19–22 frames/second (a 30 ms exposure time with a 4 × 4 binning) The W-View beam splitter contained two 510 dichroic mirrors and 480 nm and 580 nm band pass filters. For excitation of cameleons, specimens were exposed to a light with a 410 nm band pass filter and 455 nm dichroic mirror.

Image-J was used for all analysis. We determined calcium-wave rates by measuring changes in fluorescence intensity of specific regions of interest in sequential frames. The *inx-16(ox144)* wave rates are averages of data from *inx-16(ox144)* animals imaged with inverse pericam and cameleon. The rates calculated with the respective calcium indicators were very similar. For example, the “very slow” waves imaged with inverse pericam averaged 35.70 μm/s (n = 5), whereas the “very slow” waves imaged with cameleon averaged 42.53 μm/s (n = 3). To determine the correlation of muscle contraction with calcium flux, we used *inx-16(ox144)* inverse-pericam movies with slow waves that initiated in abnormal (anterior) locations because only the high magnification of the inverse-pericam imaging setup allowed us to score movement. For this analysis, the images were smoothed, and then the total area and fluorescence intensity within a region of interest was calculated in consecutive frames. The change in intestinal area is used as a measure of contraction. Contraction of the body wall muscles cannot be directly determined because the muscles are not fluorescently labeled and are not visible. Because body-muscle contraction squeezes the intestine and thus results in decreased intestinal area, we measured intestinal area. For Figure 4G, the traces were normalized to the least-square mean line fit. The relative decrease in area was inverted for reflecting increased movement. Because inverse-pericam fluorescence decreases when calcium increases, we inverted the inverse-pericam measurement to indicate a calcium

increase, making the relationship of fluorescence and calcium concentrations more intuitive.

Aldicarb Test

Aldicarb (2-methyl-2-[methylthio]propionaldehyde O-[methylcarbamoyl]oxime) was solubilized in acetone and then diluted to working stock solutions in M9. Standard NGM worm plates were treated with Aldicarb and allowed to dry at room temperature overnight. For each experiment, 20 young-adult animals were added to duplicate Aldicarb-treated plates and scored blind for paralysis after 6 hr. Results

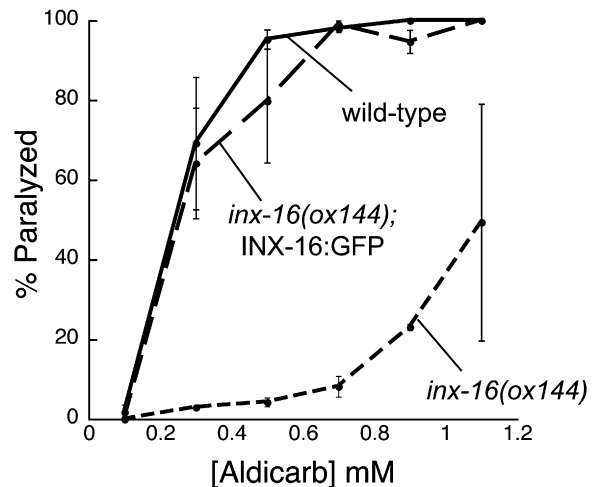


Figure S3. *inx-16(ox144)* Worms Are Resistant to the Acetylcholinesterase Inhibitor Aldicarb

Wild-type, *inx-16(ox144)*, and *inx-16(ox144)* *oxEx524* [INX-16:GFP] animals were scored blind for paralysis after a 6 hr aldicarb treatment.

from three experiments have been averaged. Error bars represent SEM.

Supplemental References

- S1. Brenner, S. (1974). The genetics of *Caenorhabditis elegans*. *Genetics* 77, 71–94.
- S2. Thomas, J.H. (1990). Genetic analysis of defecation in *Caenorhabditis elegans*. *Genetics* 124, 855–872.
- S3. Miyabayashi, T., Palfreyman, M.T., Sluder, A.E., Slack, F., and Sengupta, P. (1999). Expression and function of members of a divergent nuclear receptor family in *Caenorhabditis elegans*. *Dev. Biol.* 215, 314–331.
- S4. MacMorris, M., Broverman, S., Greenspoon, S., Lea, K., Madej, C., Blumenthal, T., and Spieth, J. (1992). Regulation of vitellogenin gene expression in transgenic *Caenorhabditis elegans*: short sequences required for activation of the *vit-2* promoter. *Mol. Cell. Biol.* 12, 1652–1662.
- S5. Adler, C.E., Fetter, R.D., and Bargmann, C.I. (2006). UNC-6/Netrin induces neuronal asymmetry and defines the site of axon formation. *Nat. Neurosci.* 9, 511–518.
- S6. Schuske, K., Palfreyman, M.T., Watanabe, S., and Jorgensen, E.M. (2007). UNC-46 is required for trafficking of the vesicular GABA transporter. *Nat. Neurosci.* 10, 846–853.
- S7. Kennedy, S., Wang, D., and Ruvkun, G. (2004). A conserved siRNA-degrading RNase negatively regulates RNA interference in *C. elegans*. *Nature* 427, 645–649.
- S8. Kamath, R.S., and Ahringer, J. (2003). Genome-wide RNAi screening in *Caenorhabditis elegans*. *Methods* 30, 313–321.